Development and Evaluation of a Prosthetic Ankle Emulator With an Artificial Soleus and Gastrocnemius

David M. Ziemnicki
Mem. ASME
Department of Mechanical Engineering,
Vanderbilt University,
2201 West End Avenue,
Nashville, TN 37235
e-mail: david.m.ziemnicki@vanderbilt.edu

Joshua M. Caputo
Human Motion Technologies LLC,
630 William Pitt Way U-PARC Building A2,
Pittsburgh, PA 15238
e-mail: josh@humotech.com

Kirsty A. McDonald
Department of Exercise Physiology,
School of Health Sciences,
University of New South Wales,
Level 2, Wallace Wurth Building,
UNSW,
Sydney, NSW 2052, Australia
e-mail: kirsty.mcdonald@unsw.edu.au

Karl E. Zelik
Department of Mechanical Engineering,
Vanderbilt University,
2201 West End Avenue,
Nashville, TN 37235;
Department of Biomedical Engineering,
Vanderbilt University,
2201 West End Avenue,
Nashville, TN 37235;
Department of Physical Medicine and Rehabilitation,
Vanderbilt University,
2201 West End Avenue,
Nashville, TN 37235
e-mail: karl.zelik@vanderbilt.edu

In individuals with transtibial limb loss, a contributing factor to mobility-related challenges is the disruption of biological calf muscle function due to transection of the soleus and gastrocnemius. Powered prosthetic ankles can restore primary function of the mono-articular soleus muscle, which contributes to ankle plantarflexion. In effect, a powered ankle acts like an artificial soleus (AS). However, the biarticular gastrocnemius connection that simultaneously contributes to ankle plantarflexion and knee flexion torques remains missing, and there are currently no commercially available prosthetic ankles that incorporate an artificial gastrocnemius (AG). The goal of this work is to describe the design of a novel emulator capable of independently controlling artificial soleus and gastrocnemius behaviors for transtibial prosthesis users during walking. To evaluate the emulator's efficacy in controlling the artificial gastrocnemius behaviors, a case series walking study was conducted with four transtibial prosthesis users. Data from this case series showed that the emulator exhibits low resistance to the user's leg swing, low hysteresis during passive spring emulation, and accurate force tracking for a range of artificial soleus and gastrocnemius behaviors. The emulator presented in this paper is versatile and can facilitate experiments studying the effects of various artificial soleus and gastrocnemius dynamics on gait or other movement tasks. Using this system, it is possible to address existing knowledge gaps and explore a wide range of artificial soleus and gastrocnemius behaviors during gait and potentially other activities of daily living.
[DOI: 10.1115/1.4052518]

1 Introduction

One of the major goals for individuals with lower-limb loss is to retain their mobility and independence in order to stay engaged in community and employment activities; however, mobility-related challenges make their physical activity more difficult and fatiguing [1–3]. In individuals with transtibial limb loss, a contributing factor is the disruption of biological calf muscle function due to transection of the soleus and gastrocnemius. Powered prosthetic ankles can restore primary function of the mono-articular soleus muscle, which contributes to ankle plantarflexion [4]. In effect, a powered prosthetic ankle could be thought of as an artificial soleus (*AS*). However, the biarticular gastrocnemius connection that simultaneously contributes to ankle plantarflexion and knee flexion torques remains missing, and there are currently no commercially available prosthetic ankles that incorporate an artificial gastrocnemius (*AG*).

Recent evidence suggests that adding an AG could improve gait mechanics of individuals with transtibial limb loss, for instance, by offloading the knee flexor muscles [5–9]. Studies that combined an AS and an AG (either powered or passive) observed a 50% reduction in the biological contribution to prosthesis-side knee flexion moment when the AG was present, compared to control trials without the AG [7,8]. This suggests that the AG may reduce knee flexor muscle demands during walking. Consistent with this implication, another study observed that most participants walking with an AS and an AG exhibited reductions in their metabolic rate during walking (between 2 and 12%, versus walking without the AG) [8]. It has also been theorized that the addition of an AG may improve the transfer of mechanical power between the prosthetic ankle and biological body segments, and that the lack of gastrocnemius-like ankle-knee coupling may limit the ability of prosthesis users to fully benefit from higher levels of power generated by robotic ankles during the push-off phase of the gait cycle [4,10].

Despite these promising results, only a relatively narrow range of AS and AG behaviors have been tested, leaving substantial knowledge gaps in how they interact to affect gait biomechanics. For example, one such gap is related to the relative importance of the AG during walking as the push-off power generated by the AS increases. Since the gastrocnemius has been implicated to play a role in the power transfer between distal and proximal body segments in the biological limb [11–13], the restoration of an AG may be more beneficial when larger push-off power is generated by the AS. However, this has not been empirically tested.

One reason for the limited investigation of AG behaviors to date may be due to a lack of a standalone prosthesis or prosthetic emulator that can be easily applied to individuals with transtibial limb loss and that can be controlled to independently modulate the AS and AG dynamics in order to explore various behaviors and their effects. Several research groups have used swappable mechanical elements (e.g., springs or pneumatic tubes) to create and test prosthetic prototypes that include an AG; however, this approach can be time-consuming when transitioning between experimental configurations, and there are limits to the different physical behaviors that can be explored [6,9]. Of the studies that explored passive or quasi-passive AG behavior, all but one used

Manuscript received May 4, 2021; final manuscript received September 15, 2021; published online October 22, 2021. Assoc. Editor: Elizabeth Hsiao-Wecksler.

passive ankle prostheses, and thus, they did not study the effect of increased AS push-off power. The remaining study used a powered AS, and evaluated the effect a quasi-passive AG has on a prosthesis user with biomimetic levels of ankle push-off power [7]. The same research group furthered this evaluation by integrating a powered AG (actuated with an off-board motor) with the same AS, resulting in a unique prosthesis that could modulate both AS and AG behaviors [8]. However, each participant had to meet with a prosthetist to create a custom, form-fitted knee orthosis that integrated the AG with their personal prosthetic socket, which adds time, cost, and complexity to the recruitment and testing process.

Our objective was to build upon prior AG research and development by creating a versatile prosthetic emulator to enable new research to explore and fill additional knowledge gaps, such as those discussed above. To this end, the goal of this work is to describe the design of a novel emulator capable of independently controlling AS and AG behaviors for transtibial prosthesis users during walking. It was desirable for this emulator to have low force tracking errors, low hysteresis (work loop) errors during passive-elastic emulation, low resistance to the user's natural leg swing, and not require custom fabrication of a knee orthosis or prosthetic socket. It was also important for the prosthesis to be lightweight to avoid confounds to gait due to carried mass or increased inertia of the leg. Finally, a design that allowed for gait analysis (e.g., using motion capture, on a force-instrumented treadmill) was also sought to enable assessment of biomechanical responses.

2 Design

We designed and built a tethered emulator that combines (i) a Humotech Caplex PRO-001 (Pittsburgh, PA) prosthetic ankle (hardware, Fig. 1) controlled by an off-board AS actuator, (ii) an AG cable that spans the prosthetic ankle and biological knee and is controlled by an off-board AG actuator, and (iii) a dual-belt, force-instrumented treadmill. The actuators were controlled by SIMULINK-based software (a modified version of HUMOTECH software). Motion capture and other gait analysis modalities (e.g., electromyography) can be used with the emulator.

Here, we summarize considerations that influenced our design and detail the hardware and software. To maximize the ability of researchers to explore different AS and AG behaviors, we sought to develop an emulator for which the dynamics could be quickly and easily reprogrammed and adjusted as necessary. Additionally, we aimed to mitigate the need for manual manipulation (e.g., swapping) of hardware components by experimenters; since this can be time-consuming and put practical limits on experimental exploration. Since the biological gastrocnemius muscle is active during the stance and preswing phases of the gait cycle but relatively inactive during swing phase [11], we desired to develop a control strategy that could exert relatively high forces (>100 N) during a "stance mode," but then exert relatively low forces (<15 N) during "swing mode" to act transparently. To leave open the possibility of using this emulator beyond level walking on a treadmill (e.g., during stair ascent/descent), we sought to design physical attachments to the body that do not impede the user's knee range of motion. Finally, to simplify and streamline the recruitment process for participants, we sought to develop an emulator that did not require the creation of a custom knee joint orthosis for each user.

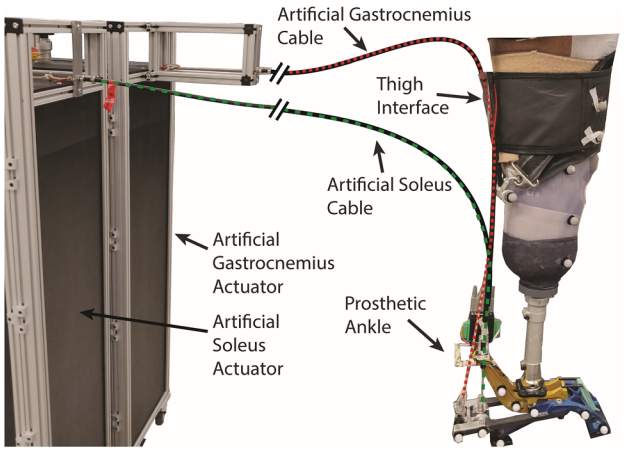

Fig. 1 Actuation and power transmission of the prosthetic emulator with an AG and an AS. A transtibial prosthesis user is shown wearing the thigh interface, which secures the AG to the leg, and the prosthetic ankle (Humotech Caplex PRO-001). The actuators drive the AG and AS Cables via Bowden cable transmission to impart torque about the participant's knee and ankle joints.

2.1 Prosthetic Ankle and Artificial Soleus. We started with a commercially available emulator, composed of a prosthetic ankle (Humotech Caplex PRO-001) and a programmable off-board motor (referred to as the Artificial Soleus Actuator, Fig. 1), that has previously shown the ability to accurately replicate powered prosthetic and biological ankle dynamics during gait [14]. The prosthetic ankle is capable of mimicking and exceeding the range of motion of the biological ankle during walking [15]. The AS actuator is connected to the prosthetic ankle via a Bowden cable transmission. It was previously shown that this type of off-board actuator system has high closed-loop torque bandwidth and is able to deliver biomimetic levels of push-off power during walking to the prosthetic ankle [14]. The AS can be programmed to control the torque-angle profile and net work generated by the prosthetic ankle for each step.

2.2 Artificial Gastrocnemius

2.2.1 AG Characteristics. We developed an AG that connects to the prosthetic ankle but is actuated independently from the AS. We established a set of AG characteristics and metrics (Table 1) to evaluate AG technical capabilities. The first two characteristics in Table 1 address the controllability of the AG while the prosthetic foot is on the ground in stance. The third characteristic addresses the control of the AG during leg swing (i.e., when low resistance is desired to avoid interfering with the user's knee flexion/extension and natural leg swing). Within this study, these characteristics are benchmarked (Results) and then discussed in the context of similar robotic emulators (Discussion).

2.2.2 AG Hardware. The AG (Fig. 1) consists of an AG actuator that pulls the AG cable to adjust tension between a thigh interface and the posterior end of the prosthetic ankle's lever. Thus, the AG simultaneously provides plantarflexion torque about the ankle and flexion torque about the (biological) knee.

The thigh interface is made of two flexible, lightweight layers that secure the AG cable to the user's body. The first layer is a 5 mm thick, 175 mm tall thermoplastic elastomer sleeve, made from a prosthetic liner (Alpha Classic, WillowWood, Mt. Sterling, OH), that fits snugly to the participant's leg above the knee. In effect, this serves to extend the length of their existing prosthetic liner. The next layer, made of nylon canvas, adheres to the thigh sleeve via hook and loop attachments and holds the AG cable conduit against the posterior aspect of the user's leg as shown in Fig. 2. By securing the conduit in this position just above the knee joint, the AG cable approximates the path of the biological gastrocnemius throughout knee flexion. This layer tightens around the leg with the use of Boa fasteners (Boa Technology, Denver, CO) that easily allow the user to tighten the interface by turning a dial, increasing the normal force against the leg. As a result, the maximum friction between the skin and the thigh sleeve increases, and the interface is capable of withstanding the AG cable forces we applied (around a maximum of 100–200 N) without sliding down

Table 1 Key AG characteristics and their associated metrics for the evaluation of the emulator's controllability in stance (force tracking and hysteresis errors) and resistance on the user's leg in swing

AG characteristic	Metric
Force tracking errors	Root-mean-square-error between measured and desired tension in stance phase
Hysteresis errors during ideal spring emulation	Difference between energy stored and energy returned during stance phase
Resistance from AG cable during swing phase	Average tension during swing phase

the leg. In addition to avoiding the need to create a custom knee orthosis to interface between the off-board motor and the body, this nonrigid interface design is low-profile, lightweight, and does not impede knee range of motion. To accommodate different user leg girths, we fabricated a number of differently sized thigh interface components.

The AG cable is a Bowden cable driven by the off-board AG actuator. The AG cable, consisting of a V-12 Vectran Single Braid 3 mm inner rope (New England Ropes, Fall River, MA), runs from the shaft of the actuator unit (shown in Fig. 3), through a flexible coiled-steel conduit (415310-00, Lexco Cable Mfg., Norridge, IL), exits the conduit at the junction held by the thigh interface, and attaches to the load cell mounted on the posterior end of the prosthetic ankle.

We customized the standard Humotech PRO-001 prosthetic ankle hardware by extending the posterior lever by approximately 4 cm to provide space for a second load cell, which enables independent measurement of AS and AG cable tensions (Fig. 3).

Regarding the ratio of the AG's moment arm at the knee versus the AG's moment arm at the ankle, we find that, depending on the size of the user's leg, the AG's knee to ankle moment arm ratio is about 0.6. This value is a reasonable approximation of the same biological ratio, which can range from 0.35 to 0.8, based on previous studies that have estimated or measured the analogous moment arms [16,17].

2.2.3 AG Control and Sensing Algorithms. The dynamics of the AG cable are programmable and therefore could take many forms (e.g., acting as a passive spring during stance or generating net positive work each step). Here, we will be discussing and evaluating a method for an ideal spring emulation in the AG cable as an example of a potential actuation pattern. The control algorithm (Fig. 4) we developed for this initial design validation study has two modes: Stance and Swing. The controller tensions the AG to impart torque about the knee and ankle while the foot is in stance, and then it reduces tension in the AG to allow the knee to extend without resistance during leg swing. In stance mode (activated when the vertical force on the treadmill exceeds a ground reaction force (GRF) threshold of 10 N), the AG actuator drives the AG cable according to the behavior prescribed by the experimenter in the software. In swing mode (activated when the vertical force on the treadmill is less than the GRF threshold), the emulator slackens the AG cable so that the participant can swing their leg forward with low resistance. Impedance control based on the work presented in Ref. [14] was used for the AS.

When Stance Mode begins, the controller utilizes proportional feedback with a desired tension of 25 N to remove any residual slack remaining from the swing phase. This tension value was informed by pilot data; it is sufficiently high to avoid load cell noise transients, yet not high enough to noticeably affect the participant's kinematics or comfort. This proportional controller persists until the angle of the prosthetic ankle reaches 2.5 deg dorsiflexion (where 0 deg represents the prosthesis being orthogonal to the pylon), typically occurring shortly after heel strike at ~12% stride. At that time, the value of the AG actuator encoder, which measures the length of the AG cable, is recorded as the spring set point of the AG cable. We selected 2.5 deg dorsiflexion based on pilot testing because it was identified as a point at which the residual slack in the biarticular cable is typically eliminated.

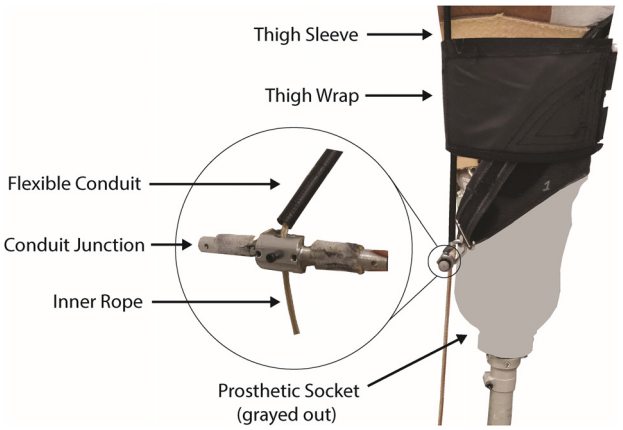

Fig. 2 Thigh interface and AG attachment. The thigh interface is a flexible, low profile accessory. It includes a thigh wrap (made of hook and loop material) that adheres to a thermoplastic elastomer sleeve, anchoring the AG cable to the participant's leg and maintaining the cable's orientation along the leg. The thigh interface also holds the conduit junction in place with straps that run up the medial and lateral sides of the leg and are secured by the thigh wrap's Boa fasteners. The flexible conduit is inserted to the junction and secured by a set screw (shown disassembled here) where the inner rope exits the flexible conduit and continues downward to connect to the load cell on the prosthetic ankle (not depicted). For image clarity, the user's prosthetic socket has been grayed out.

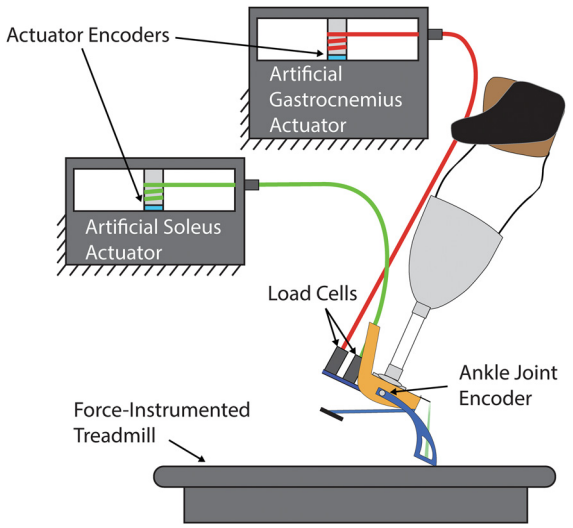

Fig. 3 Schematic of sensor instrumentation for the closed-loop control of the emulator system. Two in-line load cells measure the forces applied by the AS and AG cables to the prosthetic ankle. Two encoders measure cable displacements at the actuators. Another encoder mounted on the prosthesis measures ankle angle. A split-belt instrumented treadmill measures ground reaction forces. Closed-loop control of the AS is based on the AS load cell and the ankle joint encoder. Closed-loop control of the AG is based on the AG load cell and the encoder mounted to the AG actuator (by converting the angular displacement to linear displacement of the cable).

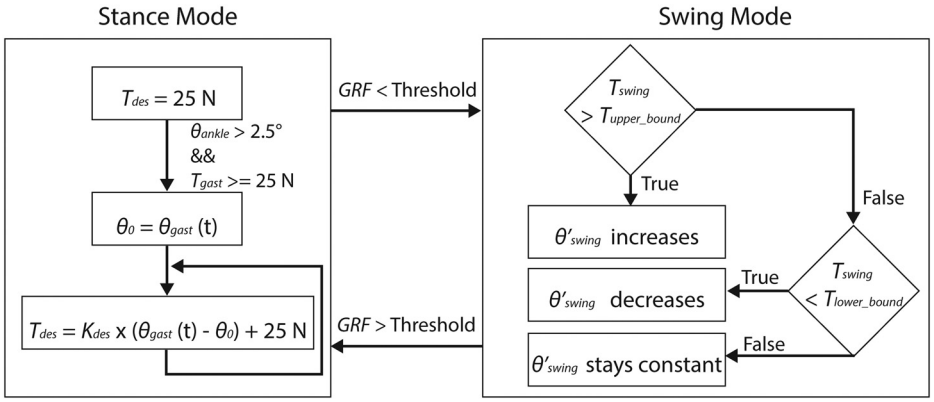

Fig. 4 Control algorithms for stance and swing modes. For the stance mode block, T_{des} is the desired tension in the AG cable, θ_{ankle} is the dorsiflexion angle of the prosthetic ankle, T_{gast} is the tension in the AG cable, θ_0 is the spring set-point, θ_{gast} is the angle of the AG encoder, and K_{des} is the desired stiffness. For the swing mode block, T_{swing} is the tension in the AG cable during the previous swing mode, and θ'_{swing} is the rate of slack that is provided during the current swing mode. GRF is the vertical component of the ground reaction force, as measured by the instrumented treadmill. Desired parameters are set by the experimenter in the software.

Additionally, by beginning the AG cable's behavior at the same kinematic configuration (prosthetic ankle angle) for each step, this helps to reduce variability in AG dynamics between strides.

The encoder on the AG actuator shaft is used to measure the linear displacement of the AG cable. As the participant progresses through stance phase, they extend their knee which imparts an extension force on the AG cable, rotating the actuator shaft and encoder. The extension of the AG cable is measured by converting the encoder's angular displacement (from the spring set point) to a linear displacement. Multiplying this extension by the experimenter's prescribed (software input) spring stiffness yields the desired tension for the AG cable at that instant. Using the load cell mounted at the posterior lever for feedback, a proportional-integral-derivative (PID) controller was used to attenuate the errors between the desired and measured tensions in the AG cable. In its simplest form, this control approach assumes that compliance in the AG cable's inner rope is negligible; an evaluation of this assumption can be found in the Discussion section.

Swing mode has two main goals related to controlling the rate of slack created in the AG cable. The first is to provide an adequate rate of slack during swing mode to allow the participant to extend their knee and swing their leg forward with negligible resistance from the AG cable. The second goal is to avoid overly high rates of slack to ensure that the cable can be quickly retensioned in early stance mode.

The controller we developed performs a calibration process during the first five steps where it evaluates the AG cable tension during Swing Mode and adjusts the rate of slack production in response. If the average AG cable tension during swing exceeds 25 N, the controller will increase the rate of slack to reduce resistance to leg swing. Conversely, if the average measured tension is below a minimum threshold of 10 N, the controller will decrease the rate of slack to keep some nominal tension in the AG and avoid leaving excess slack in the AG cable during the transition to stance mode. During this calibration process, the stance mode only controls for a desired 25 N tension and does not enforce the spring-like behavior. After the first five calibration steps, the Stance Mode spring controller is enabled and the Swing Mode will continually monitor and adjust the rate of slack provided to adapt to any changes in the user's leg swing.

3 Experimental Validation

3.1 Experimental Protocol and Data Collection. An initial case series study was conducted to evaluate the force tracking error, hysteresis error, and swing resistance (Table 1). Unilateral transtibial prosthesis users ($N = 4$; male; 34 ± 9.7 years; 1.8 ± 0.1 m; 87.6 ± 12.2 kg) were invited to attend two sessions; one familiarization session, and one data collection session at Vanderbilt University's Center for Rehabilitation Engineering and Assistive Technology. The protocol was approved by the Vanderbilt University Institutional Review Board, and all participants gave their written informed consent.

For both sessions, participants wore their prescribed socket and the experimental prosthetic ankle was fitted with a pylon that was cut to match the height of the participant's prescribed prosthetic foot (as per training and instruction by a certified prosthetist). The participants donned the AG hardware and an upper body safety harness (attached to the ceiling via a slightly slack cable).

We performed a two-dimensional parameter sweep. The AS was programmed to provide either 0.08 or 0.16 J/kg (termed *low power mode* and *high power mode*) of net work per kilogram of participant body mass to the prosthetic ankle over the course of each step. The low power mode was chosen to simulate biomimetic levels of net work and perform like the powered ankles in Refs. [7] and [18]. The high power mode was chosen to simulate these same powered ankles when tuned to provide greater amounts of net work per step, as in Ref. [19]. The AG was programmed to simulate virtual springs with stiffnesses of 0, 28, 56, and 84 N/m/kg (termed *no*, *low*, *medium*, and *high stiffness*), scaled by participant body mass such that the highest stiffness tested was roughly 8.4 kN/m. These values were determined by participant feedback during pilot testing, where participants expressed that stiffnesses beyond about 84 N/m/kg began to make walking uncomfortable; hence, we tested a range of four stiffnesses equally spaced between 0 and 84 N/m/kg. We performed the AS parameter sweep by manipulating the dorsiflexion and plantarflexion torque-angle curves in the standard HUMOTECH software. The AG stiffness sweep was performed by numerically inputting the desired stiffness into the software. All walking trials were conducted on a split-belt instrumented treadmill (Bertec, Columbus, OH), with a sampling frequency of 2000 Hz. Retroreflective markers were affixed to the prosthetic foot and the thigh interface's conduit junction, which allowed us to measure the displacement of the AG cable via motion capture, and compare this to the cable displacement measured at the AG actuator encoder.

During the first session, participants were familiarized with the prosthetic ankle and AG hardware while walking on the treadmill at 1.1 m/s; this speed was based on the reported preferred walking speed of passive prosthesis users [4] and feedback from our

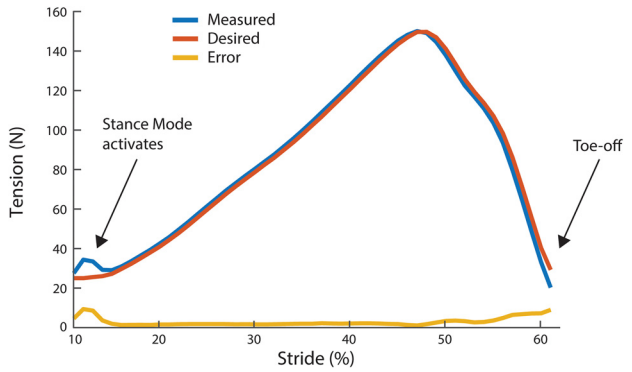

Fig. 5 A representative graph of measured and desired tension in the AG during stance mode (10–60% of stride, with a stride being defined as one foot contact to the next ipsilateral foot contact). Tension tracking maintains high accuracy during the majority of stance phase with slightly increased errors following foot contact and before toe-off when the controller switches modes.

participants during pilot testing. Participants reported that, before familiarization, they had never walked with a powered prosthetic ankle or similar AG device. They walked with each of the trial settings (a combination of the different net work values provided by the AS and AG stiffnesses; eight in total) for three minutes, allowing them to become familiar with the different behaviors of the AS and AG emulator.

With the exception of one participant who returned 16 days after their first session, other participants returned within a week of session one (3 days ± 2) for the second session where data were collected. Before beginning the data collection trials, participants completed a five-minute acclimation period where they walked at a pace of 1.1 m/s while the emulator acted as a passive AS (i.e., a torsion spring with a stiffness of 4 N·m/rad per kg of participant mass and a maximum rotation of 0.33 rad) with a no stiffness AG.

Each trial was 3 min long, and only the last 90 s of data were recorded. Trials were conducted in randomized order.

3.2 Data Processing. GRF and synchronized motion capture data (Vicon, Oxford, UK) were filtered with a zero-phase, fourth-order, low-pass Butterworth filter with a cutoff frequency of 15 and 8 Hz, respectively. Additionally, the prosthetic ankle angle, AS cable tension, AG cable length (approximated by AG actuator angle), and AG tension were recorded.

The AG tension data were filtered with a first order, low-pass Butterworth filter with a cutoff frequency of 30 Hz. We evaluated force tracking errors in the AG by computing the difference between measured and desired cable tension. The root-mean-square of these errors was then taken for each step. Hysteresis during ideal spring emulation was found by integrating the tension in the AG with respect to its extension while being stretched (during stance mode) and subtracting that value from the integrated tension while the cable was recoiling, resulting in the net work done by the AG while in ideal spring emulation. Resistance (force) from the AG during the swing phase was measured by the tension in the cable during swing mode.

4 Results

4.1 Force Tracking Error During Stance Mode. The root-mean-square-error (RMSE) between the measured and desired AG tension (Fig. 5) was 5.9 ± 0.9 N (5.6 ± 0.7% of the average maximum tension for each trial) while the prosthetic ankle was in low power mode (0.08 J/kg), and 8.2 ± 2.3 N (8.0 ± 2.1% of the average maximum tension for each trial) in high power mode (0.16 J/kg). Of the 24 trials, composed of approximately 90 strides each, only two trials exhibited average RMSE values above 10 N.

4.2 Hysteresis for Passive Spring Emulation. On average, AG hysteresis magnitudes ranged from 0.5 to 0.8 J (Table 2) where an average of 1.6 ± 0.2 J was stored in the AG cable and 1 ± 0.2 J was returned. The differences between the energy returned and stored by the AG seldom exceeded 1 J (5% of strides exceeded 1 J, 1% exceeded 1.5 J). For both low and high power AS modes, as the AG stiffness increased, the net work (hysteresis error in Joules) increased as well.

4.3 Low Resistance From AG During Swing Mode. The average tension during the swing phase across all subjects and settings was 9.8 N ± 6.4 N. The tension during swing across all subjects and settings rarely exceeded 25 N. When asked, no participant reported that they felt the AG was affecting their ability to extend their knee and swing their leg forward, which is consistent with previous findings from similar prosthetic emulators [14].

5 Discussion

We developed an experimental emulator for controlling and evaluating various AG and AS behaviors on persons with transtibial limb loss. The emulator maintains low AG tension (resistance) during swing and is capable of controlling AG tension in stance with low RMSE (5.6 ± 0.7% of the average maximum tension for each trial). This performance is comparable to that of other AGs previously used for gait studies [8,20]. The error after foot contact seen in Fig. 5, where the measured tension exceeds the initial desired 25 N, is likely due to an overshoot from the stance mode's initial proportional controller, which is corrected as the stance mode transitions to the PID controller for the simulated spring actuation. The nominal net work done by the AG (<1 J compared to the >8 J typically supplied by the AS), coupled with the low force tracking error, demonstrates that the AG is able to simulate various passive springs across a broad range of stiffness values. The low tension observed during Swing Mode operation, alongside the participants' subjective feedback confirming freedom of movement, confirmed that the AG does not impede the user's leg swing.

One unique aspect of this emulator that is worth calling attention to is the thigh interface (Fig. 2). For lab testing, this facilitates participant recruitment by providing a practical and comfortable way to anchor the AG to the user's thigh without needing to modify their socket or create a custom knee orthosis for each prosthesis user. If an AG is determined to provide sufficient mobility benefits to warrant translation beyond the lab, then this type of thigh interface might be a feasible option for an everyday use AG.

Table 2 RMSE for AG tension, and net work produced by the AG during stance mode for all power and stiffness settings

	Tension RMSE (N)		Net work produced (J)	
Spring stiffness	Low power mode	High power mode	Low power mode	High power mode
Low	6.8 ± 0.3	8.9 ± 1.8	0.7 ± 0.1	0.8 ± 0.2
Medium	5.9 ± 1.7	7.8 ± 2.4	0.5 ± 0.1	0.5 ± 0.1
High	5.0 ± 0.4	7.8 ± 2.7	0.5 ± 0.1	0.5 ± 0.1

For each trial combination, the average RMSE was observed to be below 10 N.

In addition to the interface, powered actuation or quasi-passive actuation (e.g., with a clutchable spring as in Ref. [21]) would likely be needed to meet the real-world mobility needs. But in the short-term, additional lab research is warranted to better understand benefits, drawbacks, and tradeoffs of adding an AG for transtibial prosthesis users.

There are limitations of the emulator related to the breadth of tasks that could be tested, the potential errors introduced by the compliance of the AG cable's inner rope, and the control of the AG while the AS is in high power mode. First, the current tethered configuration of the emulator (where the two large actuators serve as the AG and AS) can only facilitate experiments with tasks that require a relatively small physical volume (roughly 20 square feet around the actuators, based on the length of the Bowden cable used here), making it appropriate for stationary tasks like treadmill walking, but not for larger volume tasks like walking overground for long distances.

The second limitation is that the compliant Bowden cable dynamics between the load cell and the AG encoder can lead to some errors in the closed-loop control. In this study we estimated the displacement of the AG cable using the displacement of the AG's motor encoder. However, in postprocessing, we found 10% RMSE between motion capture and encoder displacement values. Thus, the compliance of the cable slightly lowered the effective stiffness of the AG below its desired value. Future controllers could improve on this by modeling the compliance of the Bowden cable or more directly measuring AG displacement between the thigh interface and prosthetic ankle.

Finally, although the emulator is capable of accurate AG tension tracking during walking (Fig. 5, Table 2), the current control scheme may not be appropriate for all tasks. We observed that the average RMSE of the AG slightly increased (from 5.7 to 8.7 N) when the AS was in high power mode compared to the RMSE of the AG when the AS was in low power mode. This 3 N change is small relative to the average maximum tensions of about 100–200 N, but this may be an indication that alternative control designs or PID tunings may be more appropriate as the AS increases its power output for different tasks.

One alternative approach to emulate an AG is to create a robotic knee exoskeleton, as done in Refs. [7] and [8]. However, to act like an AG this would require the knee exoskeleton to be controlled using sensor signals from both the knee and ankle, which would have complicated control for our purposes (to create a system to independently control AS and AG). The knee exoskeleton also adds mechanical bulk and complexity, which we sought to avoid with the low-profile thigh interface we developed.

6 Conclusion

We have shown that this prosthetic emulator exhibits low resistance to the user's leg swing, low hysteresis during passive spring emulation, and accurate force tracking for a range of AG and AS behaviors. The emulator presented in this paper is versatile and can facilitate experiments studying the effects of various AS and AG dynamics on gait or other movement tasks. A powered AS and quasi-passive AG (fixed stiffness during stance, near-zero stiffness during swing) were demonstrated in this study to show proof-of-concept. But the emulator allows for any combination of powered, quasi-passive, or passive AS and AG behaviors in future testing. Using this system, it is possible to address existing knowledge gaps and explore a wide range of AG and AS behaviors during gait and potentially other activities of daily living.

Acknowledgment

We gratefully acknowledge Ryan Mott, Carl Curran, and Richard Ha for their technical support in troubleshooting the Humotech hardware and software. We would also like to thank Gerasimos Bastas for his insights regarding designing for prosthesis users, Steve Collins for his input into the hardware and controls design, as well as Matthew Yandell, Stephanie Molitor, and Mohh Gupta for their research assistance and contributions to preliminary work. This material is based upon work supported by the National Science Foundation Graduate Research Fellowship Program under Grant No. 1937963. Any opinions, findings, and conclusions or recommendations expressed in this material are those of the author(s) and do not necessarily reflect the views of the National Science Foundation.

Funding Data

- National Science Foundation (NSF) (Grant No. 1705714; Funder ID: 10.13039/100000001).
- NSF Graduate Research Fellowship Program (GRFP) (Grant No. 1937963; Funder ID: 10.13039/100000082).

Nomenclature

AG = artificial gastrocnemius
AS = artificial soleus
GRF = ground reaction force
$RMSE$ = root-mean-square-error

Conflict of Interest

Joshua M. Caputo is President & CEO of Human Motion Technologies LLC d/b/a Humotech which markets wearable robotic emulator systems for use research & development. The other authors have no conflicts of interest to report.

References

[1] Torburn, L., Powers, C. M., Guiterrez, R., and Perry, J., 1995, "Energy Expenditure During Ambulation in Dysvascular and Traumatic Below-Knee Amputees: A Comparison of Five Prosthetic Feet," J. Rehabil. Res. Dev., **32**(2), pp. 111–19.

[2] Hoogendoorn, J. M., and van der Werken, C., 2001, "Grade III Open Tibial Fractures: Functional Outcome and Quality of Life in Amputees Versus Patients With Successful Reconstruction," Injury, **32**(4), pp. 329–334.

[3] Waters, R. L., Perry, J., Antonelli, D., and Hislop, H., 1976, "Energy Cost of Walking of Amputees: The Influence of Level of Amputation," J. Bone Jt. Surg. Am., **58**, pp. 42–46.

[4] Herr, H. M., and Grabowski, A. M., 2012, "Bionic Ankle–Foot Prosthesis Normalizes Walking Gait for Persons With Leg Amputation," Proc. R. Soc. B Biol. Sci., **279**(1728), pp. 457–464.

[5] Willson, A., Routson, R. L., Czerniecki, J. M., Morgenroth, D. C., and Aubin, P. M., 2015, "Towards a Biarticular Prosthesis: Simulations of Walking With a Prosthetic Gastrocnemius Spring," Northwest Biomechanics Symposium, Seattle, WA, May 1–2.

[6] Malcolm, P. S., Galle, W., Derave, D., and De Clercq, 2013, "Powered Biarticular Exoskeleton With Gastrocnemius Mimicking Configuration Produces Higher Reduction in Metabolic Cost Than Soleus Mimicking Configuration," 24th Congress of the International Society of Biomechanics (ISB 2013); 15th Brazilian Congress of Biomechanics, Natal, Brazil, Aug. 4–9.

[7] Eilenberg, M. F., Endo, K., and Herr, H., 2018, "Biomechanic and Energetic Effects of a Quasi-Passive Artificial Gastrocnemius on Transtibial Amputee Gait," J. Rob., **2018**, pp. 1–12.

[8] Eilenberg, M. F., Kuan, J.-Y., and Herr, H., 2018, "Development and Evaluation of a Powered Artificial Gastrocnemius for Transtibial Amputee Gait," J. Rob., **2018**, pp. 1–15.

[9] Willson, A. M., Richburg, C. A., Czerniecki, J., Steele, K. M., and Aubin, P. M., 2020, "Design and Development of a Quasi-Passive Transtibial Biarticular Prosthesis to Replicate Gastrocnemius Function in Walking," ASME J. Med. Dev., **14**(2), p. 025001.

[10] Zelik, K. E., Collins, S. H., Adamczyk, P. G., Segal, A. D., Klute, G. K., Morgenroth, D. C., Hahn, M. E., Orendurff, M. S., Czerniecki, J. M., and Kuo, A. D., 2011, "Systematic Variation of Prosthetic Foot Spring Affects Center-of-Mass Mechanics and Metabolic Cost During Walking," IEEE Trans. Neural Syst. Rehabil. Eng., **19**(4), pp. 411–419.

[11] Neptune, R. R., Kautz, S. A., and Zajac, F. E., 2001, "Contributions of the Individual Ankle Plantar Flexors to Support, Forward Progression and Swing Initiation During Walking," J. Biomech., **34**(11), pp. 1387–1398.

[12] Zmitrewicz, R. J., Neptune, R. R., and Sasaki, K., 2007, "Mechanical Energetic Contributions From Individual Muscles and Elastic Prosthetic Feet During Symmetric Unilateral Transtibial Amputee Walking: A Theoretical Study," J. Biomech., **40**(8), pp. 1824–1831.

[13] Bobbert, M. F., Huijing, P. A., and van Ingen Schenau, G. J., 1986, "An Estimation of Power Output and Work Done by the Human Triceps Surae Muscle-Tendon Complex in Jumping," J. Biomech., **19**(11), pp. 899–906.
[14] Caputo, J. M., and Collins, S. H., 2014, "A Universal Ankle–Foot Prosthesis Emulator for Human Locomotion Experiments," ASME J. Biomech. Eng., **136**(3), p. 035002.
[15] Brockett, C. L., and Chapman, G. J., 2016, "Biomechanics of the Ankle," Orthop. Trauma, **30**(3), pp. 232–238.
[16] Buford, W. L., Ivey, F. M., Malone, J. D., Patterson, R. M., Pearce, G. L., Nguyen, D. K., and Stewart, A. A., 1997, "Muscle Balance at the Knee-Moment Arms for the Normal Knee and the ACL-Minus Knee," IEEE Trans. Rehabil. Eng., **5**(4), pp. 367–379.
[17] Rasske, K., Thelen, D. G., and Franz, J. R., 2017, "Variation in the Human Achilles Tendon Moment Arm During Walking," Comput. Methods Biomech. Biomed. Eng., **20**(2), pp. 201–205.
[18] Gardinier, E. S., Kelly, B. M., Wensman, J., and Gates, D. H., 2018, "A Controlled Clinical Trial of a Clinically-Tuned Powered Ankle Prosthesis in People With Transtibial Amputation," Clin. Rehabil., **32**(3), pp. 319–329.
[19] Ingraham, K. A., Choi, H., Gardinier, E. S., Remy, C. D., and Gates, D. H., 2018, "Choosing Appropriate Prosthetic Ankle Work to Reduce the Metabolic Cost of Individuals With Transtibial Amputation," Sci. Rep., **8**(1), p. 15303.
[20] Kim, M., Chen, T., Chen, T., and Collins, S. H., 2018, "An Ankle–Foot Prosthesis Emulator With Control of Plantarflexion and Inversion–Eversion Torque," IEEE Trans. Rob., **34**(5), pp. 1183–1194.
[21] Yandell, M. B. J. R., Tacca, K. E., and Zelik, 2019, "Design of a Low Profile, Unpowered Ankle Exoskeleton That Fits Under Clothes: Overcoming Practical Barriers to Widespread Societal Adoption," IEEE Trans. Neural Syst. Rehabil. Eng., **27**(4), pp. 712–723.